View metadata, citation and similar papers at core.ac.uk
brought to you by CORE
provided by Shanghai Institute of Optics and Fine Mechanics,Chinese Academy of Sciences

7.3 W of single-frequency output power at 2.09 μm from an Ho:YAG monolithic nonplanar ring laser

Bao-Quan Yao,[1,3] Xiao-Ming Duan,[1] Dan Fang,[1] Yun-Jun Zhang,[1] Liang Ke,[1] You-Lun Ju,[1] Yue-zhu Wang,[1] and Guang-Jun Zhao[2,4]

[1]*National Key Laboratory of Tunable Laser Technology, Harbin Institute of Technology, Harbin 150001, China*
[2]*R&D Center for Laser and Opto-Electronic Materials, Shanghai Institute of Optics and Fine Mechanics, Chinese Academy of Sciences, Shanghai 201800, China*
[3]*Email: Yaobq08@hit.edu.cn*
[4]*Email: zhaoguangjun@163.net*

Received June 26, 2008; revised July 30, 2008; accepted August 2, 2008; posted August 7, 2008 (Doc. ID 97999); published September 12, 2008

Single-frequency output power of 7.3 W at 2.09 μm from a monolithic Ho:YAG nonplanar ring oscillator (NPRO) is demonstrated. Resonantly pumped by a Tm-doped fiber laser at 1.91 μm, the Ho:YAG NPRO produces 71% of slope efficiency with respect to absorbed pump power and nearly diffraction-limited output with a beam quality parameter of $M^2 \approx 1.1$. © 2008 Optical Society of America

OCIS codes: 140.3570, 140.3580, 140.5680.

Single-frequency lasers with high output power at wavelengths near 2 μm are required for various applications in the fields of optical metrology, high resolution spectroscopy, free-space communication, and nonlinear frequency conversion to the 3–12 μm spectral region and for measurement systems involving coherent detection. A monolithic nonplanar ring oscillator (NPRO) can combine the advantages of a pure stable single-frequency operation and a very low resonator loss [1]. Excellent open-loop frequency and power stabilities and high output power up to 3.5 W have been demonstrated for the monolithic ring design in Nd:YAG [2]. The first Tm,Ho:YAG monolithic NPRO was reported by Kane and Kubo [3] with a single-frequency output power of 31 mW. However, owing to the reabsorption losses at the quasi-three-level transition, the Tm,Ho:YAG laser was unable to reach a threshold above the temperature of 15°C. Furthermore, the cavity dimension of a few millimeters leads to a small diameter of the laser mode that is not compatible with the beam quality of the high power diodes, thus limiting the power scaling possibilities.

By use of a composite-cavity NPRO, room-temperature operation of a diode-pumped Tm:YAG laser with a single-frequency output power of 120 mW was demonstrated at 2.02 μm by Svelto and Freitag [4]. Further power scaling of monolithic NPROs is restricted by pump-light-induced thermal lensing and also stress-induced birefringence at high pump power densities [5]. A large quantum defect between the pump (785 nm) and the lasing wavelength and severe upconversion losses in Tm and Tm,Ho:YAG lead to a significantly large thermal load, which limits single-frequency lasing performance at the high power levels in room temperature. Direct (in-band) pumping of Ho:YAG with a Tm-doped fiber laser is an attractive route to high output powering the 2 μm regime, since the low quantum defect of Ho:YAG (~10%) makes the heat load small. Furthermore, the inherent high brightness available with the Tm pump source allows for a long gain medium to be used, and this provides for a distributed thermal load. Resonantly pumped Ho lasers based on a YAG host material have been extensively investigated for the generation of high power and high pulse energy 2 μm lasers by Budni *et al.* [6] and Lippert *et al.* [7].

In this Letter we demonstrate a high power monolithic Ho:YAG NPRO operating at 2.09 μm, resonantly pumped by a Tm-doped fiber laser at 1.91 μm. The 2.09 μm laser transition from Ho:YAG in our experiments, which originates from the next-to-lowest level of $^5I_7$ multiplet at ~5231 cm^{-1}, terminates at the 448 cm^{-1} sublevel of the $^5I_8$ multiplet [8]. The terminal level of $^5I_8$ manifold is ~1.8% populated at 300 K for Ho:YAG, which means that the laser is a quasi-three-level system. We estimate that only ~14.6% of the Ho^{3+} ions need to be excited for the achievement of transparency at the emission wavelength in a YAG host.

As shown in Fig. 1, the monolithic Ho:YAG NPRO has dimensions of 8 mm (width) × 10 mm (length) × 3.6 mm (height), resulting in a free spectral range (FSR) of 6.58 GHz. The input–output coupling surface of the ring resonator is plane. It is coated at point A to be 32% transmitting in *s* polarization and 67% in *p* polarization at an angle of incidence of 45°

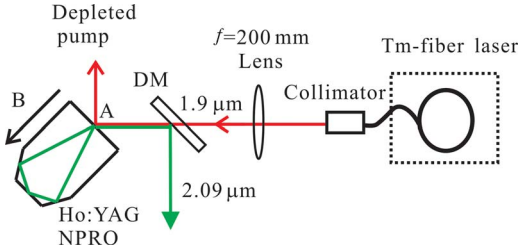

Fig. 1. (Color online) Schematic of the monolithic Ho:YAG NPRO laser end-pumped by a Tm fiber laser. DM, dichroic mirror; $T \approx 94\%$@1.9 and $R \approx 99.8\%$@2.09 μm.

 © 2008 Optical Society of America

for lasing wavelength and 88% transmitting for unpolarized pump light at 1.91 μm. For single-mode operation the crystal was placed in the field of a permanent magnet of 0.2 T average field. The differential loss between the two directions of traversal was calculated to be 0.2% by using the Jones-matrix calculus [9]. The Ho-doping concentration is 0.8 at.%, and the resonator length is about 25 mm. The optimal product of the NPRO resonator length and the doping concentration, $N_{\mathrm{Ho}} \cdot l$, is in principle determined by a trade-off between the pump absorption efficiency and the increase in laser threshold owing to the quasi-three-level nature of the laser transition. We chose $N_{\mathrm{Ho}} \cdot l = 2\% \cdot \mathrm{cm}$ in this Letter according to the analysis of Lippert *et al.* [10].

The pump source for these experiments was a Tm-doped fiber laser (Nufern LSA-TM-50 W). It provides power of 45 W cw and TEM_{00} beam quality ($M^2 < 1.3$) with 1 mm collimated output. The fiber laser is unpolarized and tuned to 1908 nm with <0.1 nm linewidth. The Tm fiber laser output was focused into the Ho laser crystal using an $f = 200$ mm lens. This focused beam was measured to have an average $1/e^2$ diameter of 0.28 mm at the location of the Ho:YAG NPRO, resulting in an estimated pump confocal parameter of greater than 80 mm inside the gain medium.

The In foil wrapped Ho:YAG laser crystal was clamped in a copper block, which was mounted onto a thermoelectric cooler (TEC) to allow for pump-generated heat removal and precise temperature control. The crystal temperature was held at 18°C. The cw single-frequency laser data obtained using this configuration are shown in Fig. 2. The highest output power was 7.3 W for 17.8 W of pump, corresponding to an optical-to-optical overall conversion efficiency of 42%. The relative laser power stability was measured to be within ±0.5% for 1 h at the highest output power level. Hops of longitudinal modes occurred and output power fluctuation increased to ±2% with more than 17.8 W of input power, although more pump power was available with the Tm-doped fiber laser. A linear regression fit to the data yields a slope of 48% and a threshold pump power of 2.3 W. The pump absorption efficiency under single-frequency lasing conditions was measured to be ~68% at any pump power

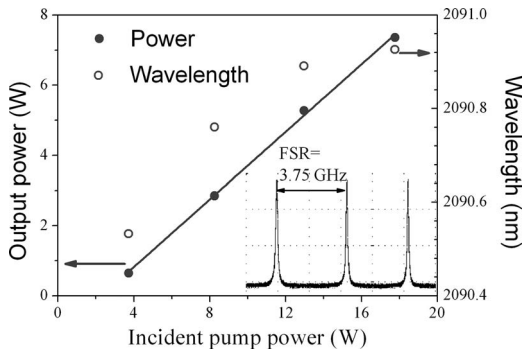

Fig. 2. Output power and wavelengths of the single-frequency Ho:YAG NPRO laser versus the incident pump power. Inset, Fabry–Perot spectrum of the single-frequency Ho:YAG NPRO laser.

levels. Corrections for absorbed pump power yielded a slope efficiency of 71% with corresponding optical-to-optical conversion efficiency of 61%. The power in the desired direction of oscillation was over 2000 times higher at the maximum output power of 7.3 W when the magnetic field was properly oriented than it was with the field reversed. The emitted radiation was elliptically polarized with a contrast ratio of 8.5 dB between s and p polarizations and corresponded to one eigenstate of the nonplanar ring laser cavity.

We measured the single-longitudinal-mode spectrum using a scanning confocal Fabry–Perot interferometer (FPI) (finesse of ~310) at the highest laser output power level, as illustrated in Fig. 2. The FSR of the FPI was approximately 3.75 GHz, as indicated in Fig. 2. The absence of any peaks between the main resonances of the interferometer clearly indicates the operation on one single longitudinal and transverse frequency.

The spectral output of the Ho:YAG NPRO laser was recorded with a Burleigh WA-650 spectrum analyzer combined with a WA-1500 wavemeter (0.7 pm resolution). The emission line is centered on 2090.9 nm at the maximum output power of 7.3 W, and no other emission oscillates with it simultaneously (Fig. 3). As shown in Fig. 2, the emission wavelengths from the Ho:YAG NPRO are redshifted from 2090.53 to 2090.93 nm with an increase of output power from 0.7 to 7.3 W. In our experiment, the temperature of the Ho:YAG crystal was controlled by driving the current of TEC and monitored by a thermistor in contact with the copper block. The laser single-frequency tuning range was investigated experimentally by changing the crystal temperature. Figure 4 shows the lasing frequency of the Ho:YAG NPRO as a function of temperature. The frequency tuning range of the laser is from 143.3800 to 143.3841 THz, which is over 4 GHz without longitudinal mode hopping between 15.6°C and 18.4°C and corresponds to the wavelength, which varies from 2090.895 to 2090.835 nm. The temperature tuning corresponds to a rate of −1.5 GHz, which is in reasonable agreement with the calculated value of −1.7 GHz/°C according to the formula [3]

$$\mathrm{d}f/\mathrm{d}T = -f[(1/n)\mathrm{d}n/\mathrm{d}T + \alpha], \tag{1}$$

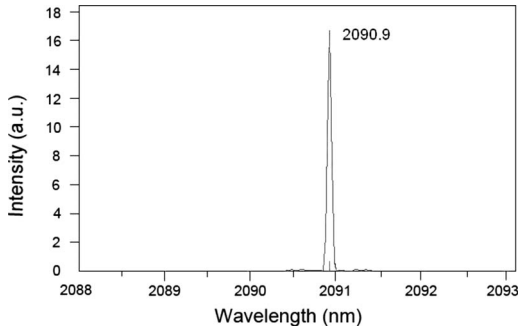

Fig. 3. Output spectrum of single-frequency Ho:YAG laser.

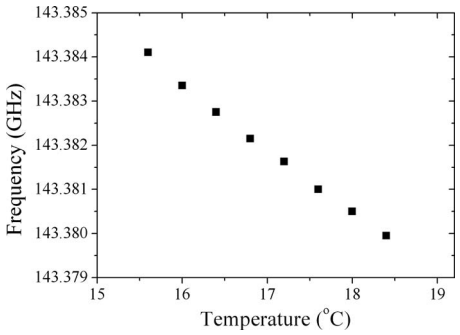

Fig. 4. Ho:YAG NPRO laser frequency as a function of temperature at 17.8 W incident pump power.

where f is the lasing frequency, n (1.8) is the index of refraction of the YAG host at 2.09 μm, dn/dT ($9 \times 10^{-6}/°C$) is the variation of the refractive index with temperature, and α ($7 \times 10^{-6}/°C$) is the thermal expansion coefficient [11]. It can also explain the redshift phenomenon of output wavelengths for the monolithic Ho:YAG laser (Fig. 2), which results from pump-induced thermal effects. With an increasing absorbed pump power, the temperature rise of the Ho:YAG crystal along the axis of the pump beam occurs based on the thermal model of end-pumped solid-state lasers of Innocenzi *et al.* [12].

As shown in Fig. 5, we measured the output beam propagation by measuring the beam radius with a knife-edge technique at several positions through a waist formed by a lens ($f = 200$ mm). The data were fitted by least-squares analysis to standard mix-mode Gaussian beam propagation equations to determine the beam quality, or M^2, parameter. The curve fit to the data yielded a nearly diffraction-limited beam with $M^2 = 1.08 \pm 0.04$.

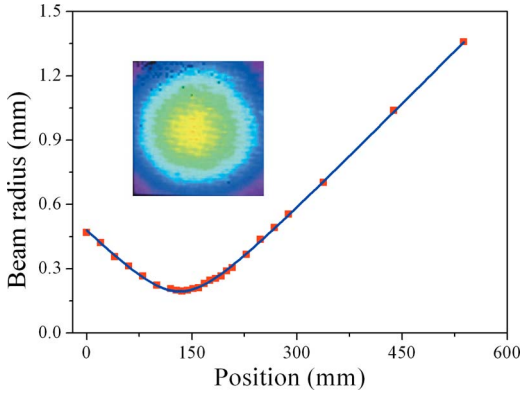

Fig. 5. (Color online) M^2 measurement of the Ho:YAG NPRO laser at output power level of 7.3 W. Inset, typical two-dimensional beam profiles taken by a Spiricon Pyrocam I pyroelectric camera.

In conclusion, single-frequency output power of as high as 7.3 W with $M^2 \approx 1.1$ from a Ho:YAG NPRO laser was achieved. The reduced pump-light-induced thermal aberrations owing to the low quantum defect of Ho:YAG and the highly bright Tm fiber laser are significantly favorable for mode-hop-free output at high power levels. A high-power single-frequency laser operating in the 2.1 μm regime can be used to drive cw optical parametric oscillators for which pump sources with high amplitude and frequency stability are required.

This paper was supported by the program of excellence team in Harbin Institute of Technology, China.

References

1. T. J. Kane and R. L. Byer, Opt. Lett. **10**, 65 (1985).
2. H. Zimer and U. Wittrock, Opt. Lett. **29**, 1635 (2004).
3. T. M. Kane and T. S. Kubo, in *Advanced Solid State Lasers*, G. Dube, ed., Vol. 6 of OSA Proceedings Series (Optical Society of America, 1990), paper ML3.
4. C. Svelto and I. Freitag, Electron. Lett. **35**, 152 (1999).
5. I. Freitag, A. Tünnermann, and H. Welling, Opt. Commun. **115**, 511 (1995).
6. P. A. Budni, M. L. Lemons, J. R. Mosto, and E. P. Chicklis, IEEE J. Quantum Electron. **6**, 629 (2000).
7. E. Lippert, S. Nicolas, G. Arisholm, K. Stenersen, A. S. Villanger, and G. Rustad, Proc. SPIE **6397**, 639704 (2006).
8. J. B. Gruber, M. E. Hills, M. D. Seltzer, S. B. Stevens, C. A. Morrison, G. A. Turner, and M. R. Kokta, J. Appl. Phys. **69**, 8183 (1991).
9. A. C. Nilsson, E. K. Gustafson, and R. L. Byer, IEEE J. Quantum Electron. **25**, 767 (1989).
10. E. Lippert, S. Nicolas, G. Arisholm, K. Stenersen, and G. Rustad, Appl. Opt. **45**, 3839 (2006).
11. R. Wynne, J. L. Daneu, and T. Y. Fan, Appl. Opt. **38**, 3282 (1999).
12. M. E. Innocenzi, H. T. Yura, C. L. Fincher, and R. A. Fields, Appl. Phys. Lett. **56**, 1831 (1990).